



PROCUREMENT EXECUTIVE, MINISTRY OF DEFENCE

AERONAUTICAL RESEARCH COUNCIL

REPORTS AND MEMORANDA

# Fan Supersonic Flutter: Prediction and Test Analysis

By D. G. HALLIWELL

Rolls-Royce (1971) Limited

LONDON: HER MAJESTY'S STATIONERY OFFICE

1977

£3 net

# Fan Supersonic Flutter: Prediction and Test Analysis

By D. G. HALLIWELL  
Rolls-Royce (1971) Limited

---

*Reports and Memoranda No. 3789\**  
*November, 1975*

---

## Summary

The subject is introduced by describing the aerodynamic and vibration characteristics of unstalled, supersonic flutter in fan assemblies having part-span shrouds or clappers. It is briefly compared and contrasted with stall flutter. The importance of frequency and modeshape analyses is stressed and supersonic flutter prediction methods are examined, commencing with the modeshape parameter  $C\theta/H$ . Unsteady work theory leads to the study of aerodynamic damping with the prediction of flutter mode, speed and wave direction. Throughout, emphasis is given to the support of design analysis by test data, from laboratory measurements on stationary models to full scale engine Altitude Test Chamber behaviour. Finally, the effect on flutter of some of the operating criteria in engine service is considered.

---

\* Replaces A.R.C. 36 374

## LIST OF CONTENTS

1. Introduction—Characteristics of Flutter
  - 1.1. Aerodynamic Limitations
  - 1.2. The Importance of Supersonic Flutter
  - 1.3. Vibration Characteristics
2. Frequency and Modeshape Analysis
  - 2.1. Assembly Frequencies
  - 2.2. Vibration Modeshapes
3. Coupled Flutter Parameter,  $C\theta/H$
4. Analytical Flutter Prediction
  - 4.1. Unsteady Work
  - 4.2. Aerodynamic Damping
5. Flutter Test Data
  - 5.1. Sea Level
  - 5.2. Altitude Simulation
6. Service Margins and Concluding Remarks

References

Illustrations—Figs. 1 to 15

Detachable Abstract Cards

## 1. Characteristics of Flutter

### 1.1. Aerodynamic Limitations

In turbofan compressors there are two principal types of aerodynamically excited instability which are of practical consequence. These are:

(a) Stall Flutter

This occurs over a band of speed just below, but usually not extending to, design speed itself. It is commonest among (although not confined to) fan or front stage compressor aerofoils of the cantilever-bladed or unclappered type. On a compressor test rig it can be observed as a blade instability which is excited when the exit throttle is closed at constant speed, and may prevent a true surge point from being attained. It is associated with a critical combination of local aerofoil stalling and blade frequency parameter.

(b) Supersonic Unstalled Flutter

This type of excitation presents a stress boundary in the high speed regime of the compressor, where the blade inlet relative velocities are well supersonic over the outer section, and where blade incidences are well away from stalling values. It is usually associated with high tip speed, high aspect ratio fans, with part-span shrouds or clappers on the blades, where the whole rotor is caused to vibrate as an integral assembly when the critical speed is reached. This is a result of work transfer from air to blade, instead of *vice-versa*; an associated change in overall performance is not discernible, however, at the maximum safe operating stress level.

A satisfactory fan design such as shown in Fig. 1 will have this flutter boundary sufficiently far above its design speed to allow for:

- (i) the highest permissible engine rating in service;
- (ii) foreseeable thrust growth by throttle opening;
- (iii) frequency and vibration modeshape variation between nominally identical fans;
- (iv) stress variation from blade to blade.

The slope of the stress boundary relative to pressure ratio may prevent the maximum flow points of the highest speed characteristics from being obtained. Typically, as shown in Fig. 1, the variation in flutter speed between open throttle and near to surge is of the order of 10 per cent.

### 1.2. The Importance of Supersonic Flutter

Unlike stall flutter, which it may be possible to accelerate through if the working line is not too high, unstalled supersonic flutter presents an operational barrier as evidenced by the stress levels shown in Fig. 1. Prolonged operation, even on the edge of this boundary is a potential recipe for disaster.

Therefore, in the remainder of this paper only the unstalled case will be dealt with. Fortunately, it is a less complex situation to predict analytically than is stall flutter, and empirical correlations have always had to be relied upon to avoid the latter. However, even when stall flutter is present, unless it is a particularly severe case, there are well-tried methods such as blade stagger increase to suppress it. There are no such ready techniques to overcome supersonic flutter and expensive mechanical redesign may be the only remedy.

### 1.3. Vibration Characteristics

In the case of fans with cantilevered blades, the vibration frequencies are governed by the blades themselves, in comparison with which the disc is extremely rigid. For a clappered fan the vibration modes are much more complex, and the presence of the clapper provides a high degree of coupling between torsion and flap modes of the blades. The vibration of such an assembly manifests itself as a series of discrete frequencies related by particular groups or families.

A representative frequency diagram is shown in Fig. 2. First and second family frequencies are relevant, these being distinguished by the number of circumferential nodes. Within a family, each vibration mode is characterized by a discrete number of radial nodes which, when excited while the fan is running, form a rotating pattern with respect to the rotor. Thus each blade experiences a constantly varying degree of torsion ( $\theta$ ) and flap ( $H$ ).

At a given instant in time, the vibration pattern of a 4-diameter mode appears as in Fig. 3. The  $\theta$  and  $H$  components are approximately 90 degrees out of phase, with the direction of rotation of the pattern dependent upon the sign of this angle. Moreover, each blade will be out of phase with its neighbours by an amount

depending upon the numbers of blades and diametral nodes. The magnitude of this angle is critical in determining which vibration mode will be the most flutter prone.

The second family of modes is usually the most important for flutter and, returning to Fig. 2, a typical case of supersonic flutter is shown in a 4D mode at about 105 per cent speed. This selection of a single dominant mode is typical of unstalled flutter, although the simultaneous presence of an adjacent mode of lower stress is not unknown. By contrast, stalled flutter on a clappered fan can cause a range of modes to be excited, say 2D to 6D.

We shall see later the reasons for the selection of a unique mode in supersonic flutter.

## 2. Frequency and Modeshape Analysis

### 2.1. Assembly Frequencies

The accurate prediction of assembly frequencies and blade modeshape is the cornerstone of any flutter prediction procedure. The static frequency prediction can be checked by vibrating a rotor assembly in the laboratory; the blade roots in the disc and the clapper faces must first be bonded together (or loaded by shims) to simulate dynamic stiffening.

More importantly, the design speed frequency prediction can be checked from the recordings of blade strain-gauges during rig or engine testing.

Flutter is not necessary for their detection as several quiescent modes are usually discernible over a wide speed range from the processed gauge signals. The location of resonance points where a given mode coincidences in frequency with its shaft order counterpart, and comparison with static frequencies enables these modes to be identified.

A comparison of test data with frequency prediction is illustrated in Fig. 4 for a typical fan. The comparison is close, except perhaps for the higher order, less important, modes.

### 2.2. Vibration Modeshapes

Under static conditions in the laboratory the vibration of a fan can be studied conveniently by the use of laser holography. A coherent light beam enables a time-averaged hologram of a vibrating rotor to be made. An example of such a hologram is seen in Fig. 3 for a 4D second family mode, in which the radial nodes appear as white lines. Because the amplitude of a blade is proportional to the number of fringes, a full vibration pattern can be built up.

Fig. 5 shows the variation of twist ( $\theta$ ) with radius at a nodal position and also the variation of deflection normal to the blade chord ( $H$ ) at an anti-node. The closeness of test and theory is encouraging, particularly in the location of the circumferential node point where the  $H$ -term changes sign. The importance of this point in determining the unsteady work transfer between air and blade will be seen later.

The extension of this technique to the rotating fan case is an order of magnitude more difficult. Ref. 2, for example, describes attempts at experimenting with reflecting areas on the blade surface in conjunction with a sophisticated pulse laser. However, useful results may be obtained by a simpler approach. At RR we have successfully used a high-speed cine-camera to photograph the motion of the blade tips of a research fan during supersonic flutter. The variation in blade stagger angle for one complete revolution of the fan is shown in Fig. 6; the upper graph is during flutter at about 200 MPa maximum alternating stress, the lower graph is just before flutter onset. The cyclical blade motion is clear, and with a knowledge of frequency, the mode number and inter-blade phase angle can easily be verified.

## 3. Coupled Flutter Parameter $C\theta/H$

A useful means of comparing the behaviour in different modes and of comparing one fan with another is the  $C\theta/H$  parameter, where  $C$  (Chord),  $\theta$  and  $H$  are defined at the blade tip section. Indeed, prior to the development of unsteady work analysis for unstalled flutter, clappered fans were designed on this basis.

The variation of  $C\theta/H$  with mode number and speed is shown in Fig. 7. The static prediction is well upheld by the holographic data already referred to and also by blade tip microscope measurements. The increasing degree of torsion in the motion as mode number increases can be seen, while the effect of speed is observed to be significant for only the higher order modes. Thus, credence is lent to the modeshape calculation procedure.

Various fans are compared in Fig. 8 for vibration in second family modes at their respective design speeds, where  $\lambda$  is the mode frequency parameter. Theory predicts that, at a given  $\lambda$ , the higher  $C\theta/H$  becomes (i.e. the greater the torsional component) then the less stable is the fan. Also, a low frequency parameter tends

towards instability. In fact, the stability boundary is a near-rectangular hyperbola relating reduced velocity ( $2\pi/\lambda$ ) and  $C\theta/H$ .

Actual test experience is shown by the solid points indicating modes where flutter has occurred. By and large, the expected boundary shape is borne out, and one should design for the likely flutter mode to lie well to the left of this boundary to be safe.

However, the draw-back to this procedure is that there is no method of knowing in advance in which mode flutter will occur, and the division between conservation and risk at the design stage becomes blurred. Indeed, from Fig. 8 it is not clear why flutter does not occur in the higher diametral modes.

## 4. Analytical Flutter Prediction

### 4.1. Unsteady Work

The basis of the unsteady work method has been outlined in other papers (e.g. Refs. 1 and 2) and will not be duplicated here, but instead some results will be explored. As well as a good definition of blade modeshape behaviour which we have already dealt with, a knowledge of the unsteady lift and moment forces acting upon the blades during free oscillation is required, and an ability to deal with these forces for different vibration modes. For blades with high Mach Number, low-camber, high-stagger tip sections, such as front fan stages, it is found that the supersonic flow, flat-plate theory developed at Cambridge (Ref. 3) gives good results.

It is first necessary to refer to the unsteady work equation itself, given by Fig. 9. This is seen to contain 3 major terms: a bending component dependent upon  $H$  only; a torsion component dependent upon  $\theta$  only; and a cross-coupling component containing both  $H$  and  $\theta$ .

It is instructive to plot each of these work components against fan radius as shown in Fig. 10. Positive work represents work transfer from the air to the blade, i.e. instability, and it can be seen that it is the cross-coupling term which is the dominantly unstable component, with the bending term counteracting this. The point where the cross-coupling term changes sign corresponds to the node of the  $H$  component referred to earlier in Fig. 5. The accuracy of location of this point when integrating the unsteady work is clearly important.

The work transfer of this cross-coupling term is found to increase rapidly with increasing mode number, as shown in Fig. 11, where each work component has been integrated up the blade. Likewise, the stabilising effect of the bending component also increases. Although the torsion component is small, it should not be neglected because, where the cross-coupling and bending terms are similar in magnitude, the torsion term can tilt the balance between stability and instability.

### 4.2. Aerodynamic Damping

So far, it has not been possible to see which particular mode will be preferred in flutter. To do this, we have to examine the logarithmic decrement of the aerodynamic damping ( $\delta_a$ ) in each mode. This is found by relating the integrated unsteady work to the kinetic energy of blade vibration. A negative value of  $\delta_a$  represents a divergent or potentially unstable system. Whether flutter actually occurs or not when  $\delta_a$  is negative depends upon the magnitude of the small but important mechanical damping of the system ( $\delta_m$ ) in relation to  $\delta_a$  (Ref. Fig. 9).

The variation of  $\delta_a$  with frequency parameter and second family mode number is shown in Fig. 12 for a given fan, operating at 100 per cent speed at sea level static (note that this may be a considerably higher speed than a normal engine take-off application). Two cases are shown, for forward and backward travelling waves relative to the rotor; the wave direction depends upon the sign of the phase relationship ( $\phi$ ) between  $\theta$  and  $H$  wave motions. For the forward wave,  $H$  leads  $\theta$  in time, for which  $\phi = -90$  deg. Fig. 12 shows this as the least stable of the two waves.

Fig. 12 also shows that instability is most likely in a middle order mode, probably the 4D case. As for the effect of speed, all that can be said at this stage is that flutter could be expected in the region of 100–110 per cent speed, depending upon the magnitude of  $\delta_m$ . In the next section we will see how these predictions compare with test data.

## 5. Flutter Test Data

### 5.1. Sea Level

We have already seen in Fig. 2 a conventional frequency diagram constructed from blade strain-gauge signals. It is equally possible to construct such a diagram for frequencies defined relative to the fan casing, and this is shown in Fig. 13 for the second family modes of the above fan. The two sets of frequencies correspond to

potential forward and backward travelling flutter patterns relative to the rotor. By means of pressure transducers located in the casing, it is possible to record the frequency of the moving pressure pattern and hence confirm its mode number and direction.

Flutter points from various tests are shown in Fig. 13 by the solid symbols. It is seen that:

- (a) flutter has occurred in the 4D mode;
- (b) the unstable wave is forward travelling;
- (c) flutter speed is generally in the 100–110 per cent regime.

Thus on each count the prediction of section 4.2 has been verified.

## 5.2. Altitude Simulation

Accumulated test data from overspeeding tests in an Altitude Test Chamber have made possible the study of the effect of flutter of a wide range of simulated flight altitude, forward speed and intake temperature. It is found that low altitude, high flight  $M_n$  and low  $T_1$  each reduces flutter speed—that is, flutter speed is inversely related to air density.

This is illustrated by Fig. 14 in which reduced velocity ( $1/\lambda$ ) is plotted against the mean air density at the fan front face. Each symbol represents a flutter test point at various intake conditions. A general speed-density trend is evident, but the effect of intake temperature is found to be more powerful than would be expected from the associated density change alone. This accounts for the majority of scatter in the test data of Fig. 14. Clearly, the calculation of the aerodynamic coefficients must be sophisticated enough to take account of this effect if the prediction is to be extended to other conditions.

As yet, a full off-design analysis of aerodynamic damping has not been performed, but because  $\delta_a$  is directly proportional to air density, its variation at flutter onset can be studied. This is shown in Fig. 15, where  $\delta_a$  is plotted against Mach Number relative to the blade tip, with density varying between S.L. take-off and high altitude cruise values. The shaded zone shows where flutter has been identified during the testing already referred to. This confirms two things:

- (a) mechanical damping is indeed significant having a value in the region of 0.002 to 0.005 depending upon density.
- (b) apart from a possible but unusual high flight  $M_n$ , low altitude case, sea level testing can be relied upon to produce the lowest flutter speed, when aerodynamic damping is negative.

## 6. Service Margins and Concluding Remarks

In conclusion, a few words should be said about flutter margins in service, because this is what really matters in the end. We have seen that sea level static flutter testing is a valuable step in clearing a fan for service operation, and the ability to predict the flutter condition is an important addition to the design process. However, unless a fan has been very conservatively designed, it is necessary to examine the in-flight margin between flutter onset and maximum engine rating speed, at critical points in the flight envelope.

This involves several other aspects of the problem which can only be touched upon, such as: the degree of flat rating of the engine; the climb-altitude schedule; the type of intake behind which an engine is to operate; overspeed during governor failure; and so on.

These factors can vary for different aircraft applications of the same engine and therefore form a separate subject in themselves. However, they are some of the more practical aspects to be borne in mind in applying the fan supersonic flutter work described in this report to engine operation in service.

### Acknowledgement

The author wishes to thank Rolls-Royce (1971) Ltd., for permission to publish this paper. Views expressed therein are his own and are not necessarily endorsed by the company.

## REFERENCES

- | <i>No.</i> | <i>Author(s)</i>  | <i>Title, etc.</i>   |
|------------|---|--|
| 1          | F. O. Carta .....   | Coupled blade-disc-shroud flutter instabilities in turbojet engine rotors.<br><i>Journal of Engineering for Power</i> , Vol. 89, July 1967, pp. 419-426. |
| 2          | A. A. Mikolajczak, R. A. Arnoldi, L. E. Snyder and H. Stargardter ... | Advances in fan and compressor blade flutter analysis and predictions.<br><i>Journal of Aircraft</i> , April 1975, pp. 325-332.                          |
| 3          | T. Nagashima and D. S. Whitehead ...                                  | Aerodynamic forces and moments for vibrating supersonic cascades of blades.<br>CUED/A-Turbo/TR 59, 1974.   |



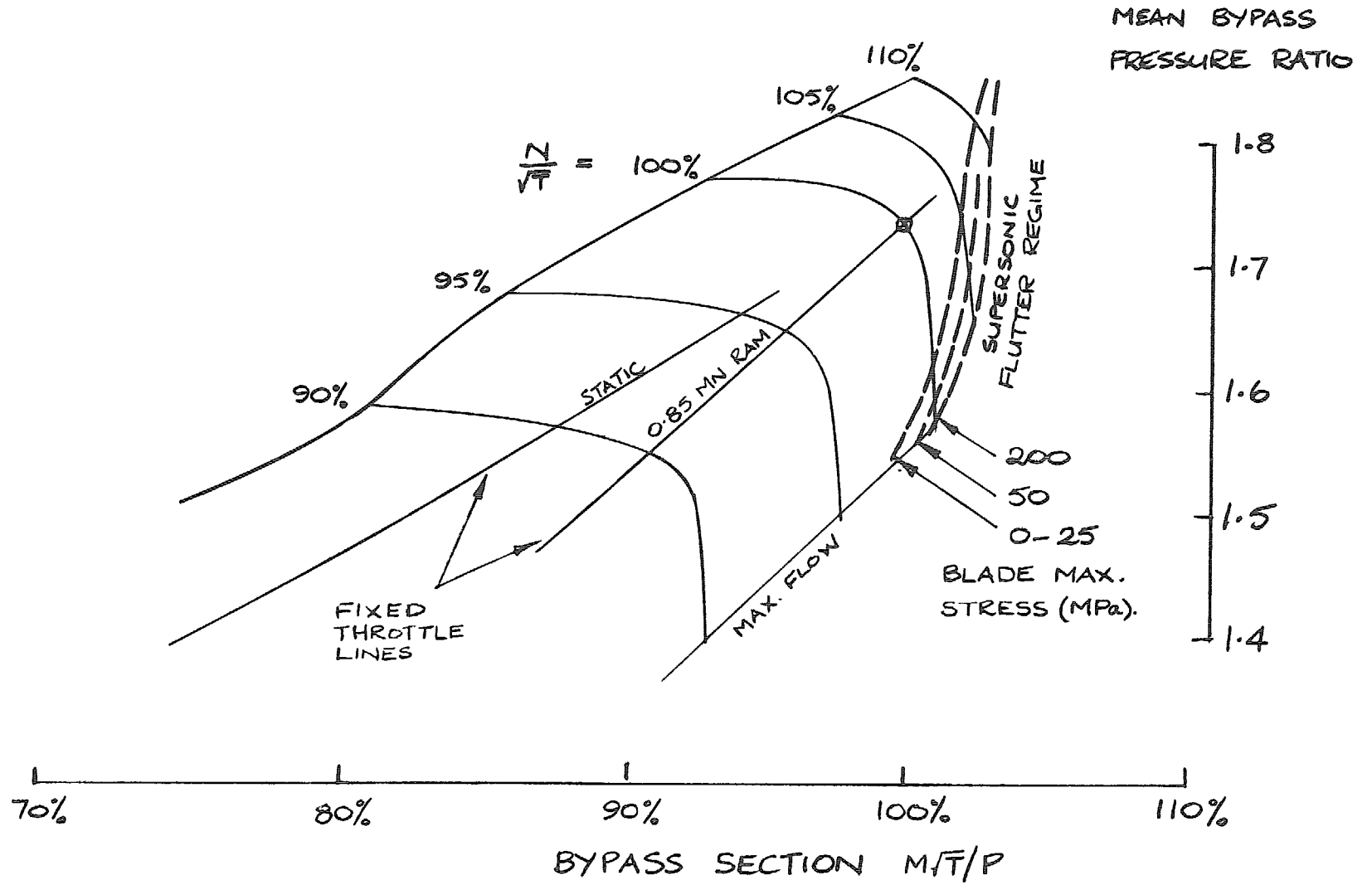


FIG. 1. Model fan characteristics showing stress boundaries of unstalled supersonic flutter.

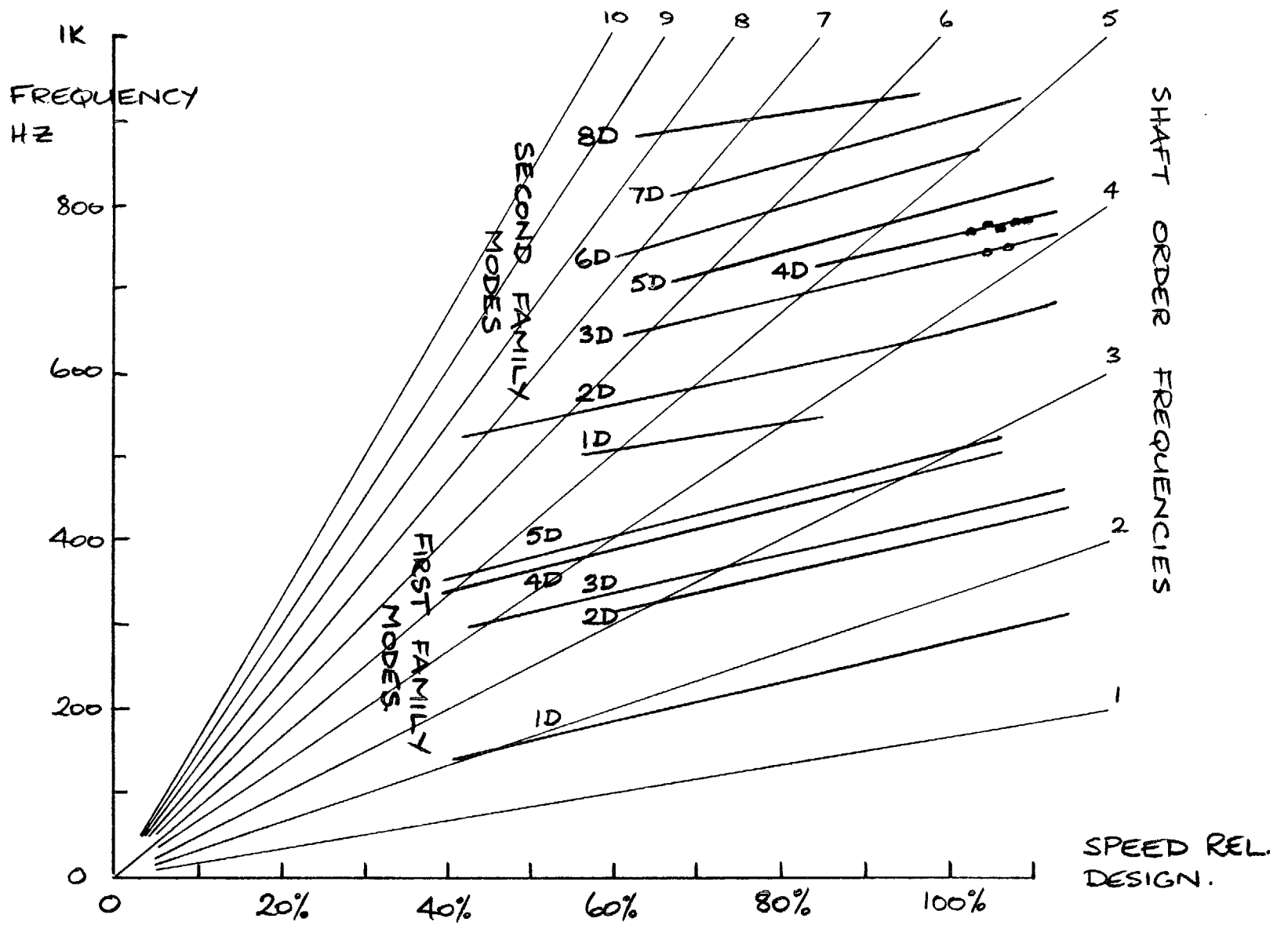
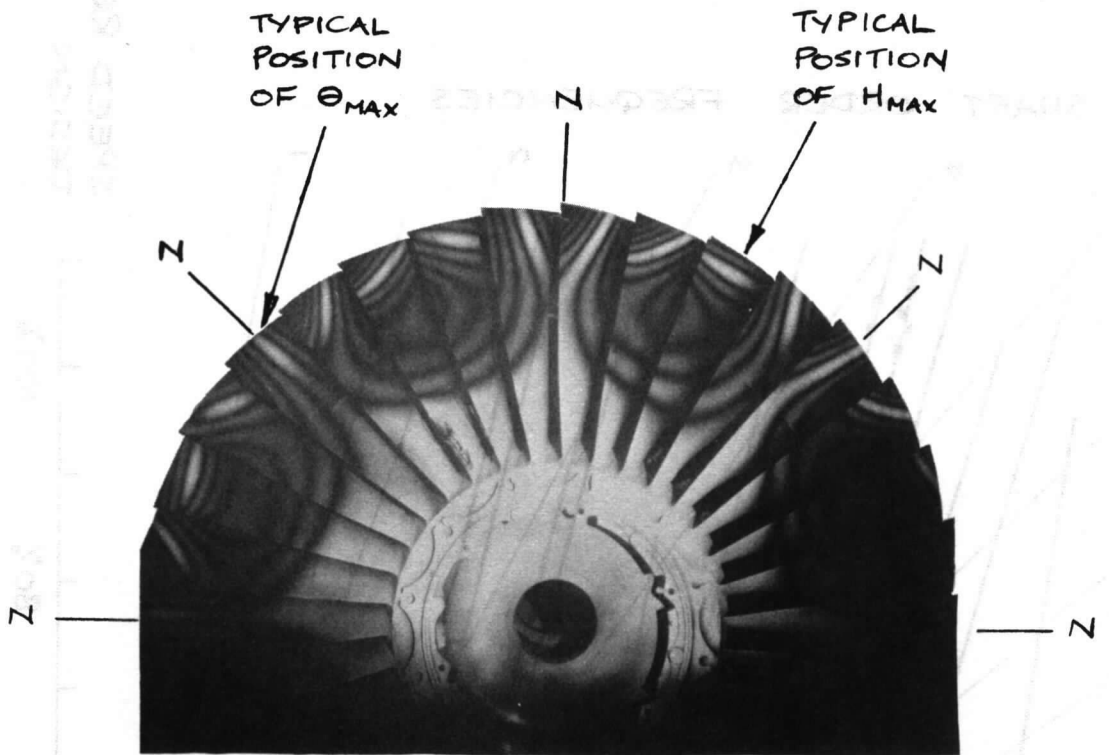
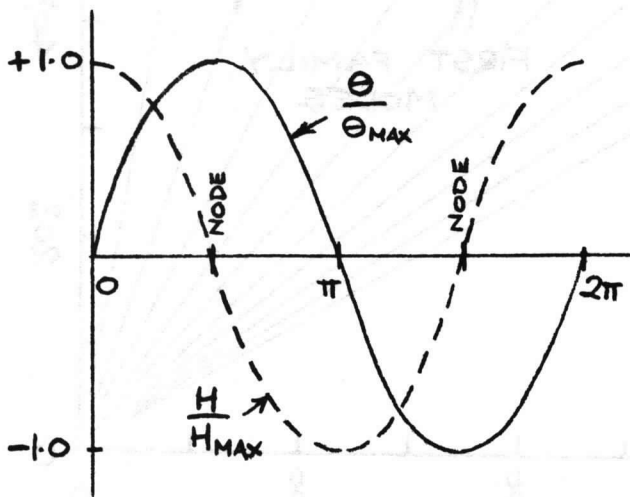


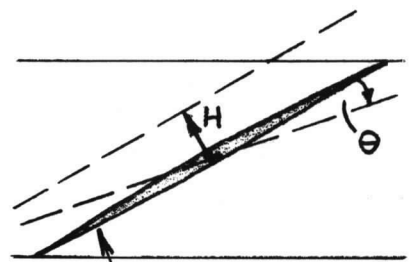
FIG. 2. Clappered fan frequency diagram.



HOLOGRAM OF 4-D ASSEMBLY MODE



VIBRATION CYCLE NEAR BLADE TIP.



UNDISTURBED BLADE POSITION VIEWED AT TIP SECTION.

FIG. 3. Fan assembly vibration modeshape definitions.

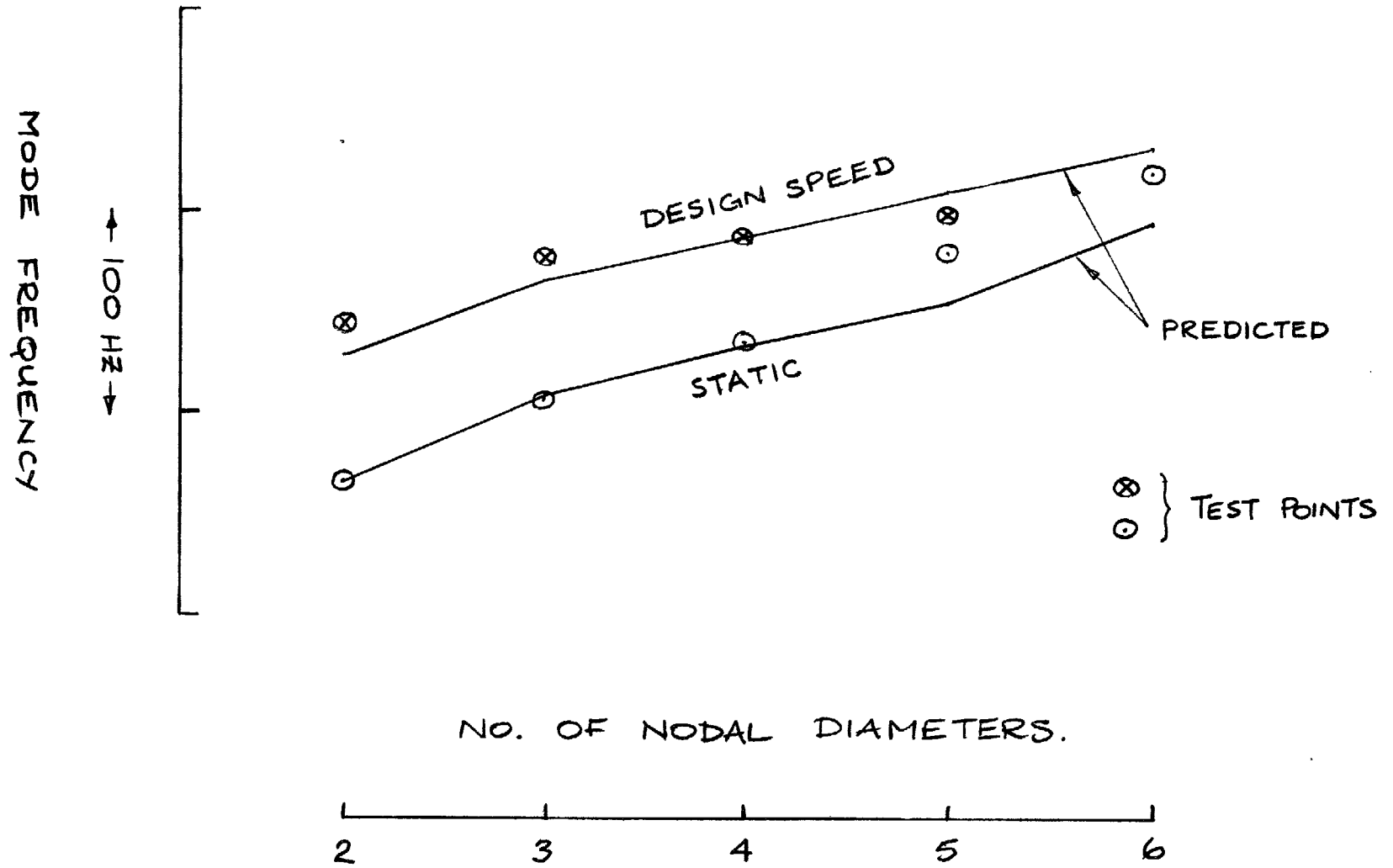


FIG. 4. Typical fan assembly frequencies. Second family modes.

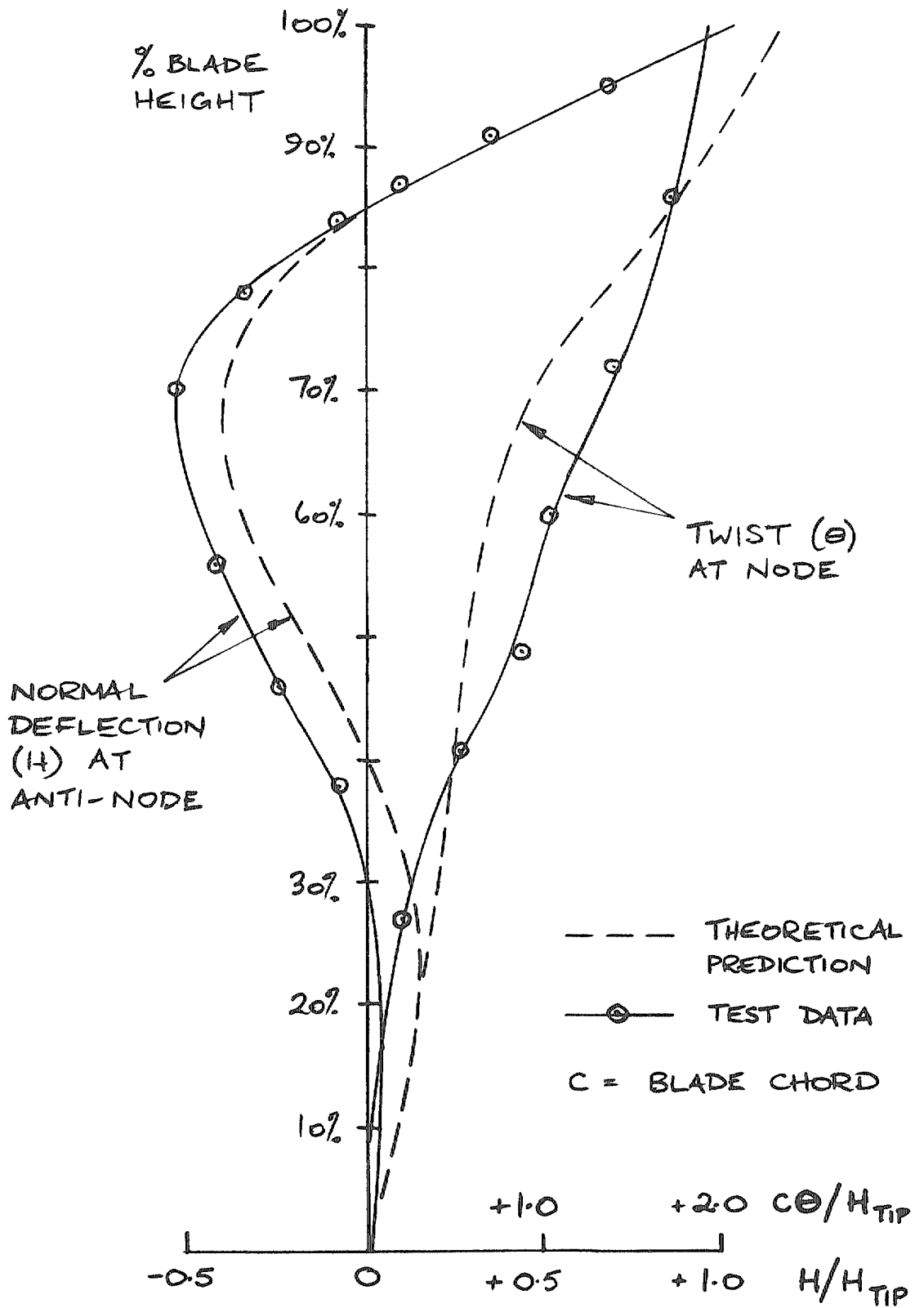


FIG. 5. Fan blade vibration prediction (4D, 2F mode) compared with holographic measurements.

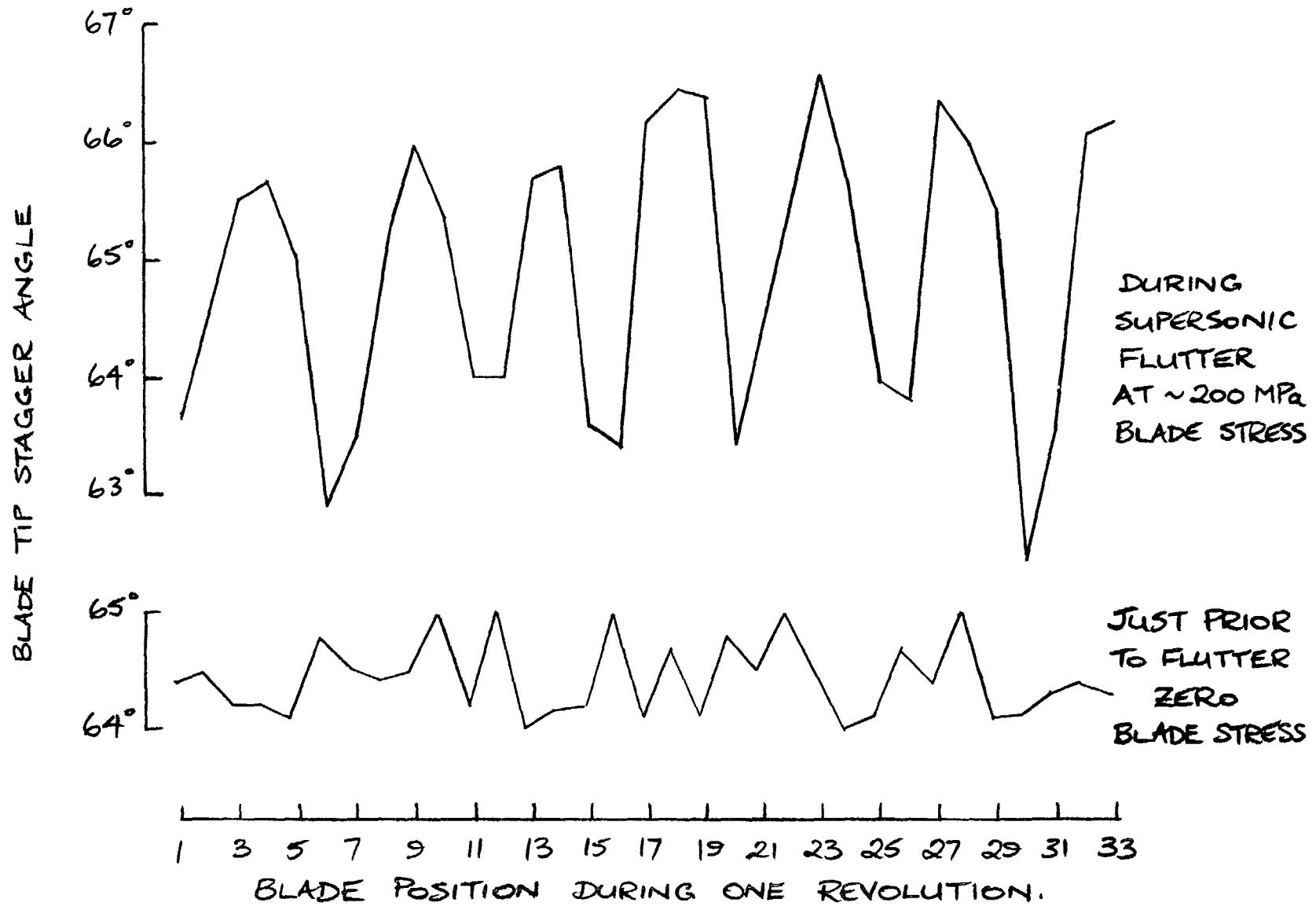


FIG. 6. High speed fan results: blade stagger variation during flutter.

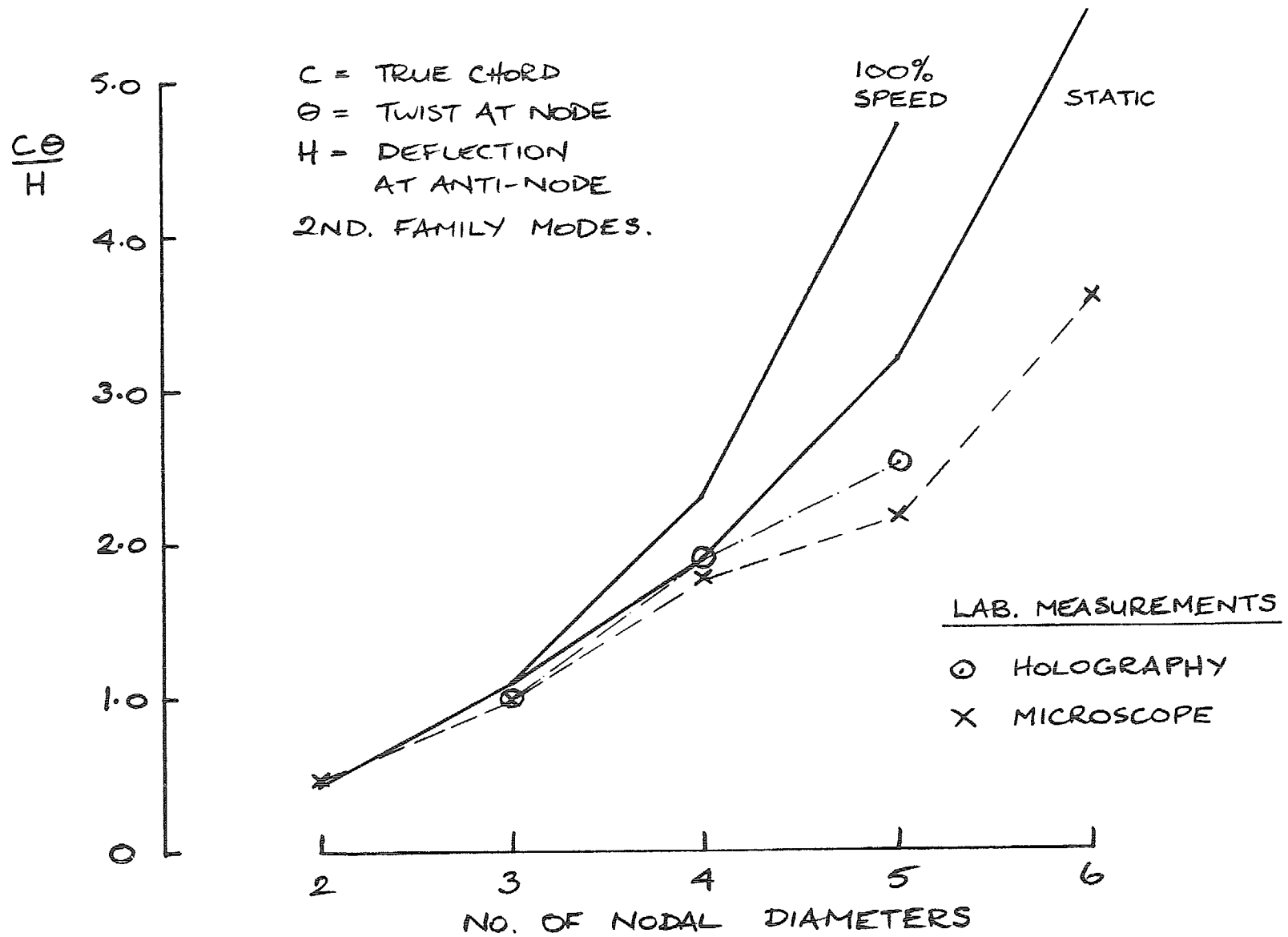


FIG. 7. Comparison of fan modeshape parameter theory and static measurements.

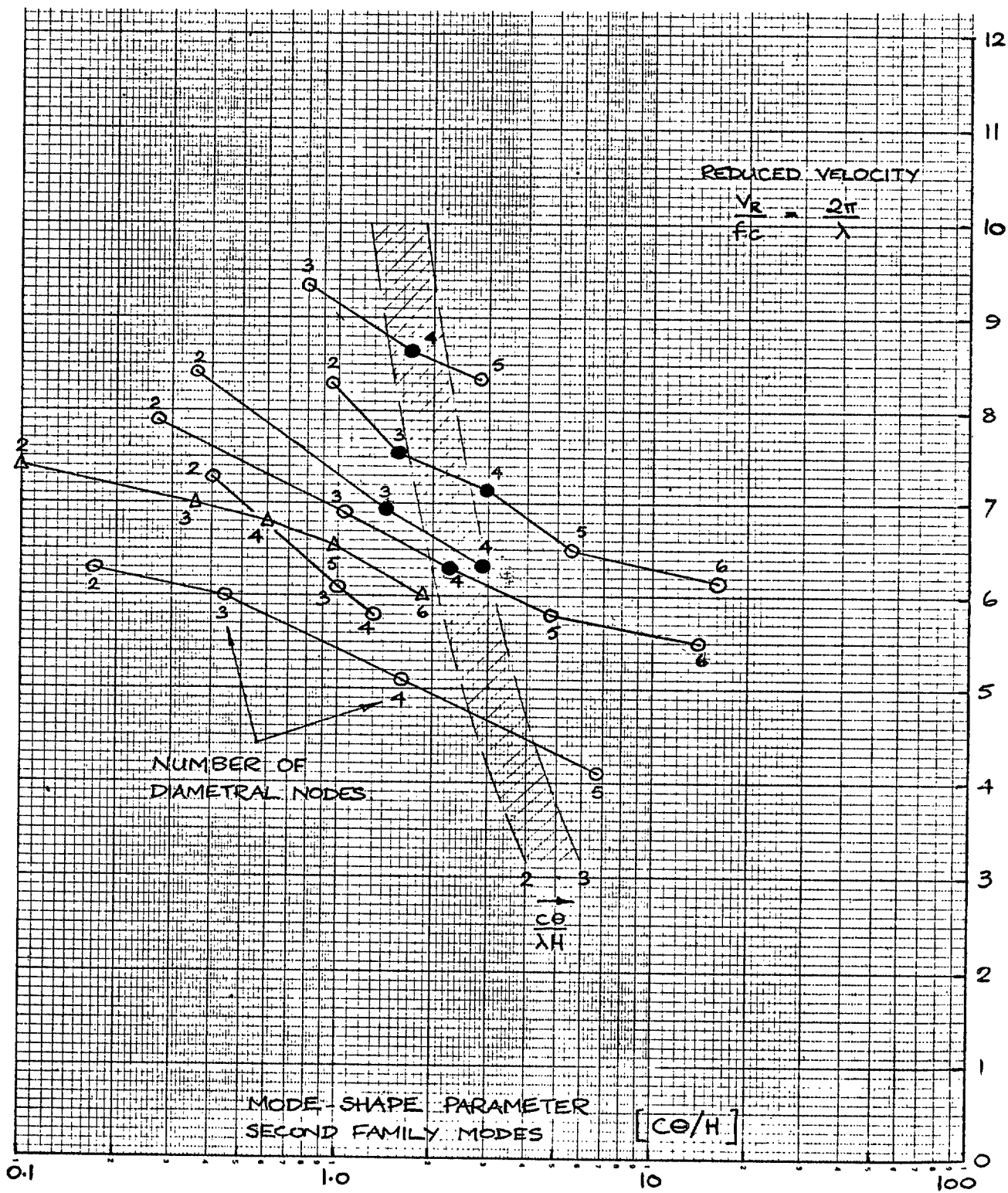


FIG. 8. Use of  $C\theta/H$  parameter for flutter prediction of clappered fans.



SYMBOLS:

$\rho_0$	AIR INLET DENSITY
$V$	BLADE REL. VELOCITY
$C$	BLADE TRUE CHORD
$\omega$	ANGULAR FREQUENCY
$r$	BLADE RADIUS.
$H$	BLADE NORMAL BENDING
$\theta$	BLADE TWIST
$P$	BLADE FORCE COEFF.
$\delta$	DAMPING LOG. DEC.
$W$	UNSTEADY WORK

SUFFIXES:

$a$	AERODYNAMIC
$m$	MECHANICAL
$L$	LIFT FORCE
$M$	MOMENT FORCE
$b$	DUE TO BENDING
$t$	DUE TO TORSION.

UNSTEADY WORK

$$W = \pi \rho_0 V C \omega \int_{r_1}^{r_2} \left[ P_{Lb} \bar{H}^2 + (P_{Mb} + P_{Lt}) C \bar{\theta} \bar{H} + P_{Mt} (C \bar{\theta})^2 \right] dr$$

AERO. DAMPING

$$\delta_a = \frac{-W}{4 \times \text{BLADE K.E. OF VIBRATION}}$$

STABILITY CRITERION

$$\delta_a + \delta_m \neq 0$$

FIG. 9. Flutter theory definitions.

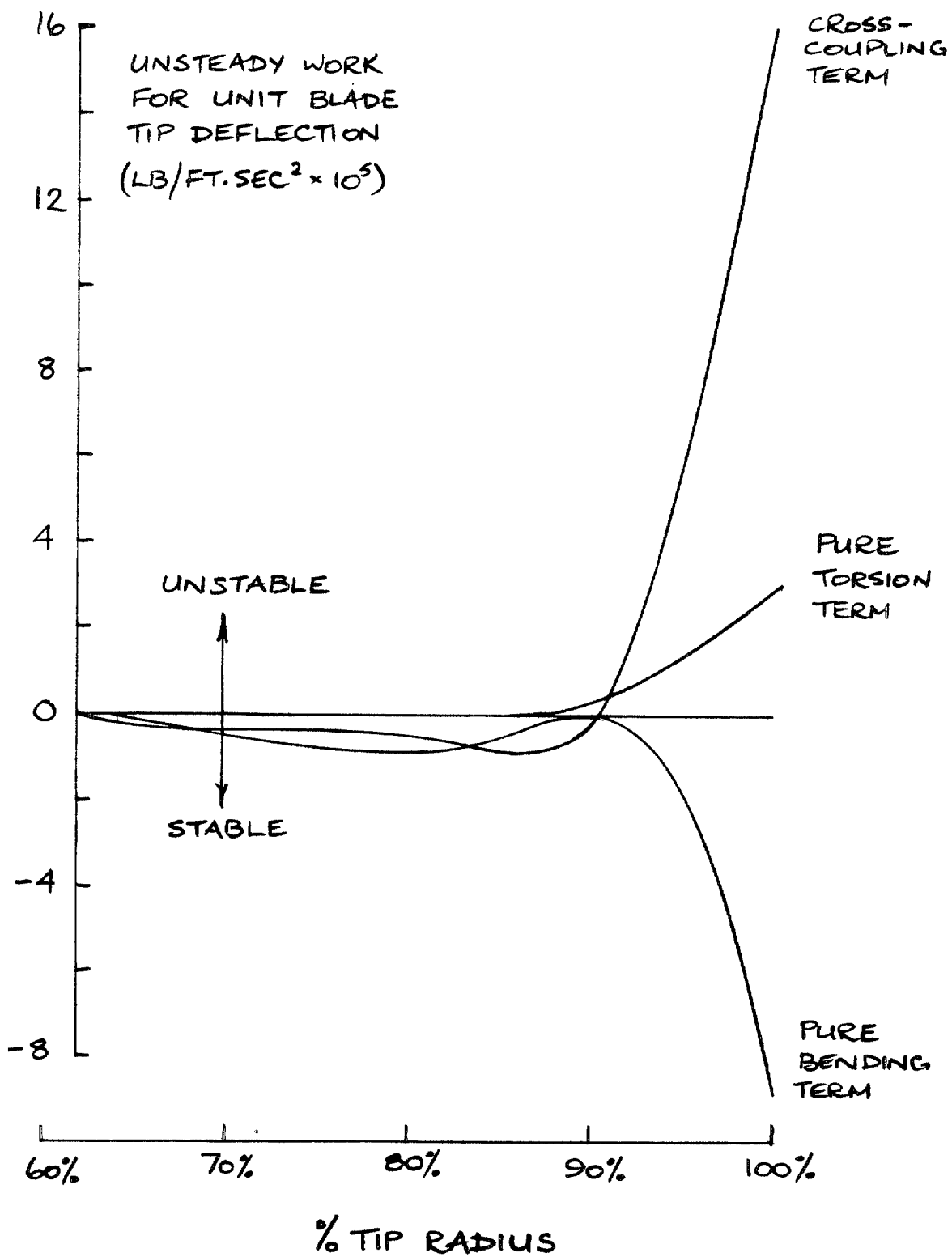


FIG. 10. Fan unsteady work components at 100 per cent speed four-diameter second family mode.

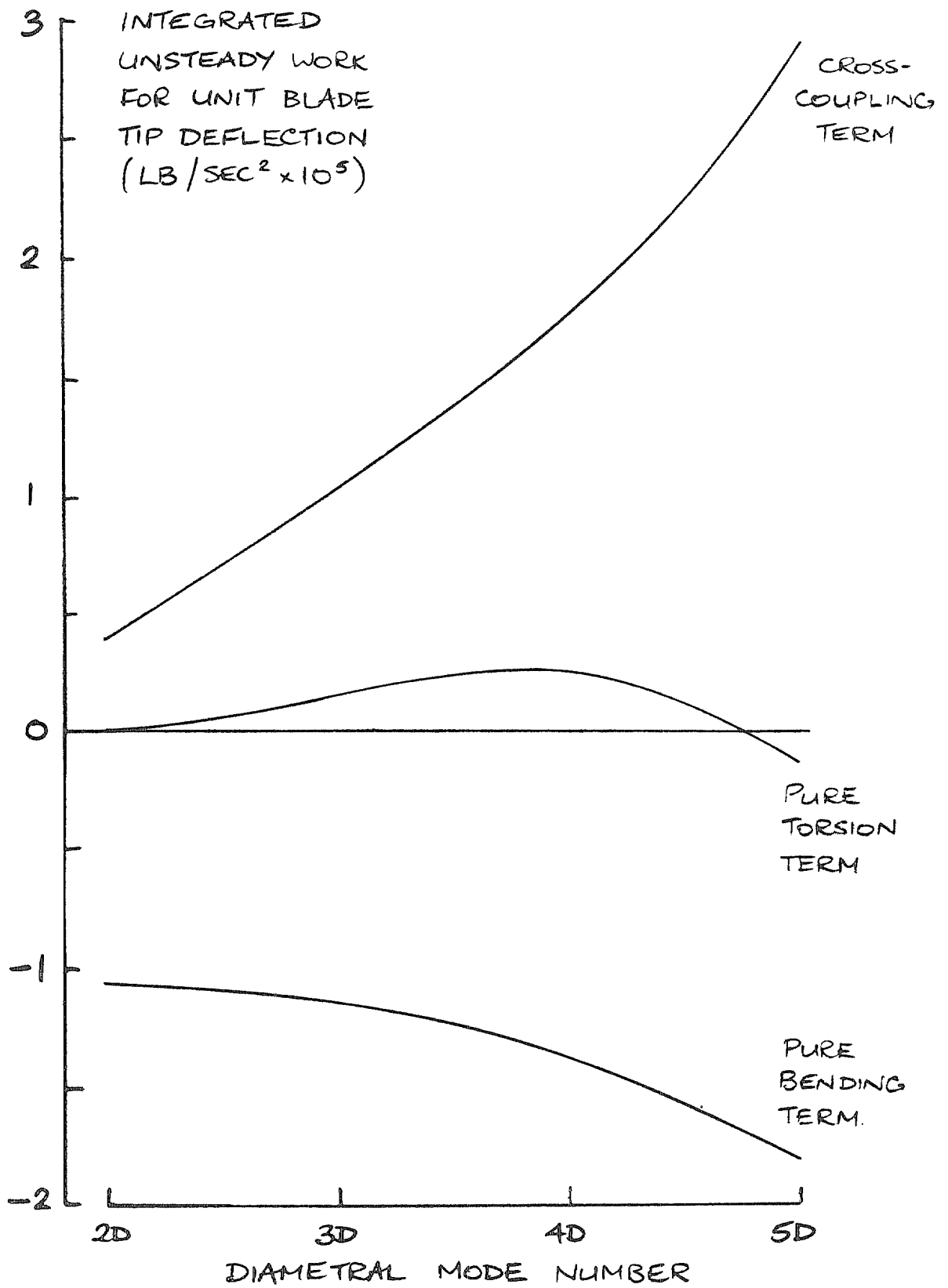


FIG. 11. Fan unsteady work components at 100 per cent speed variation with second family mode number.

# AERODYNAMIC DAMPING ( $\delta_a$ )

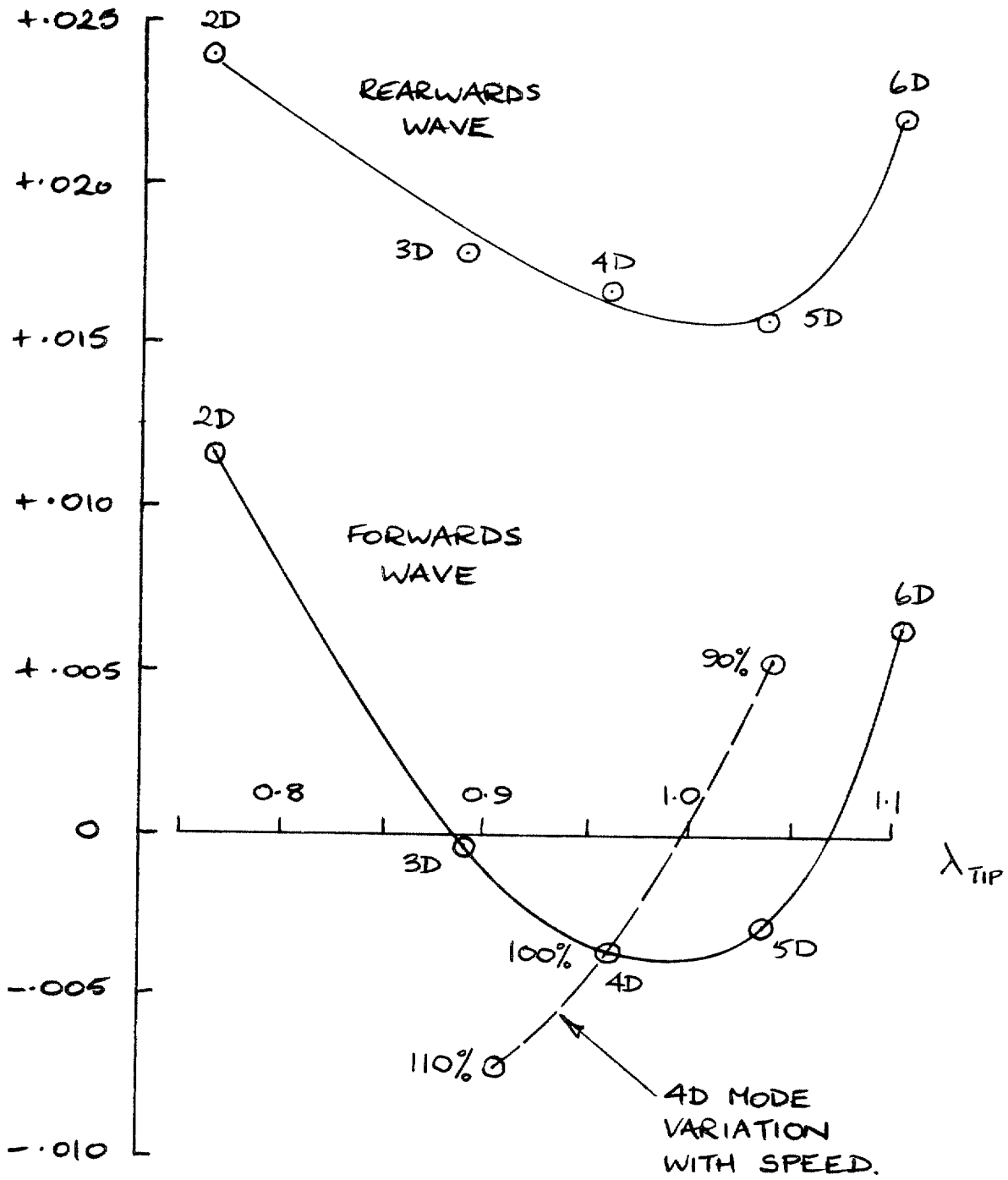


FIG. 12. Variation of fan aerodynamic damping with speed and mode number.

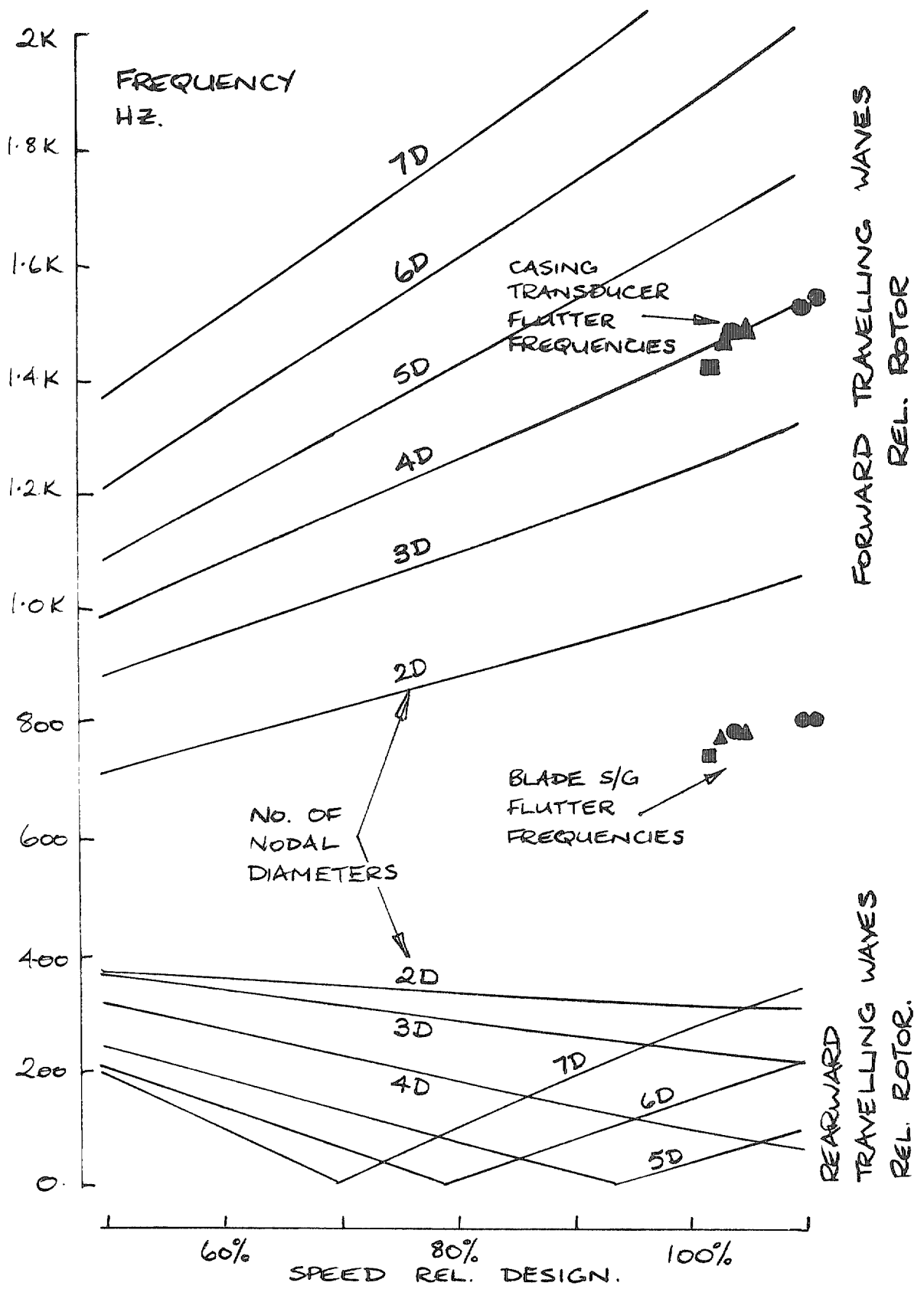


FIG. 13. Potential vibration modes (second family) defined relative to casing.

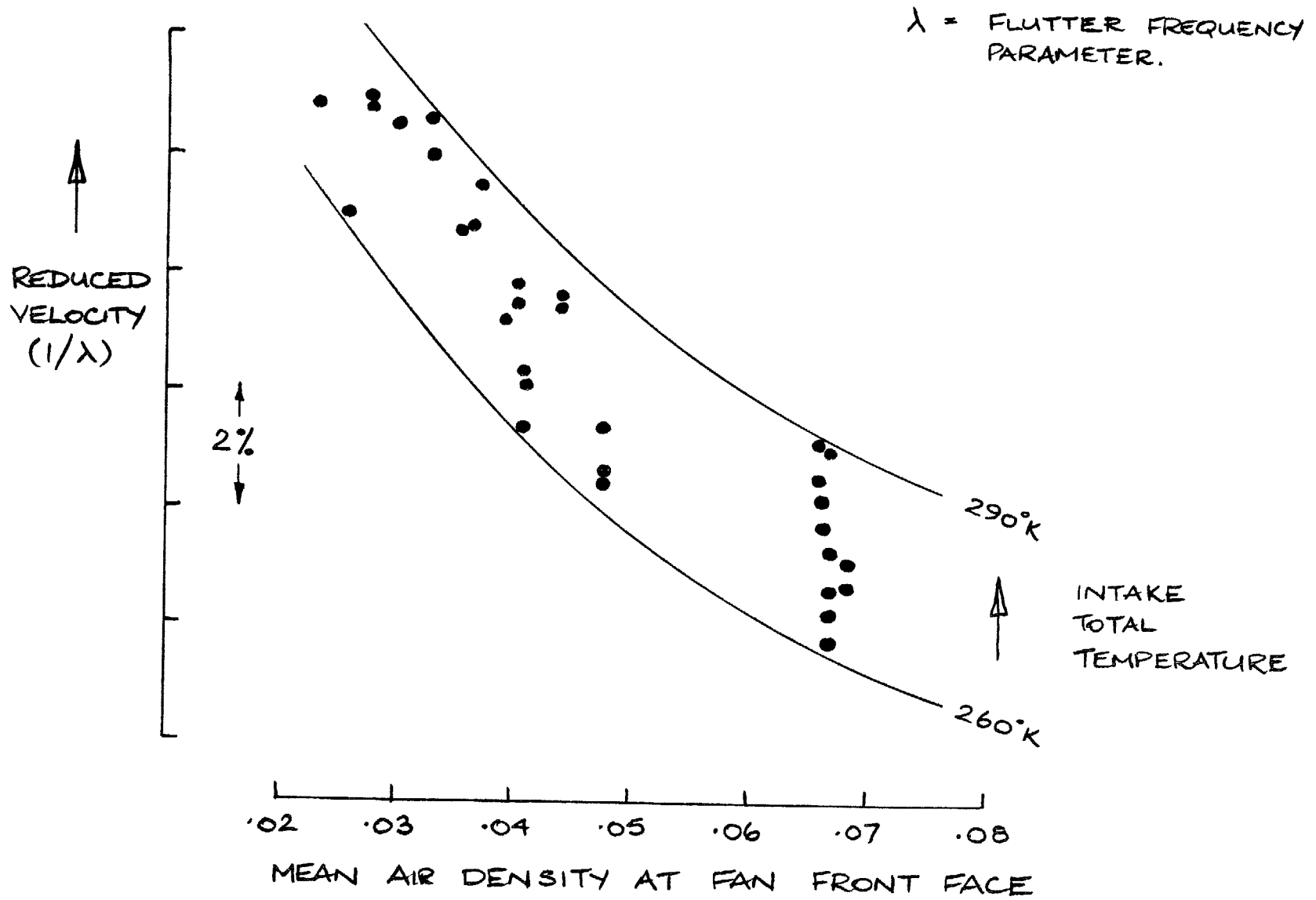
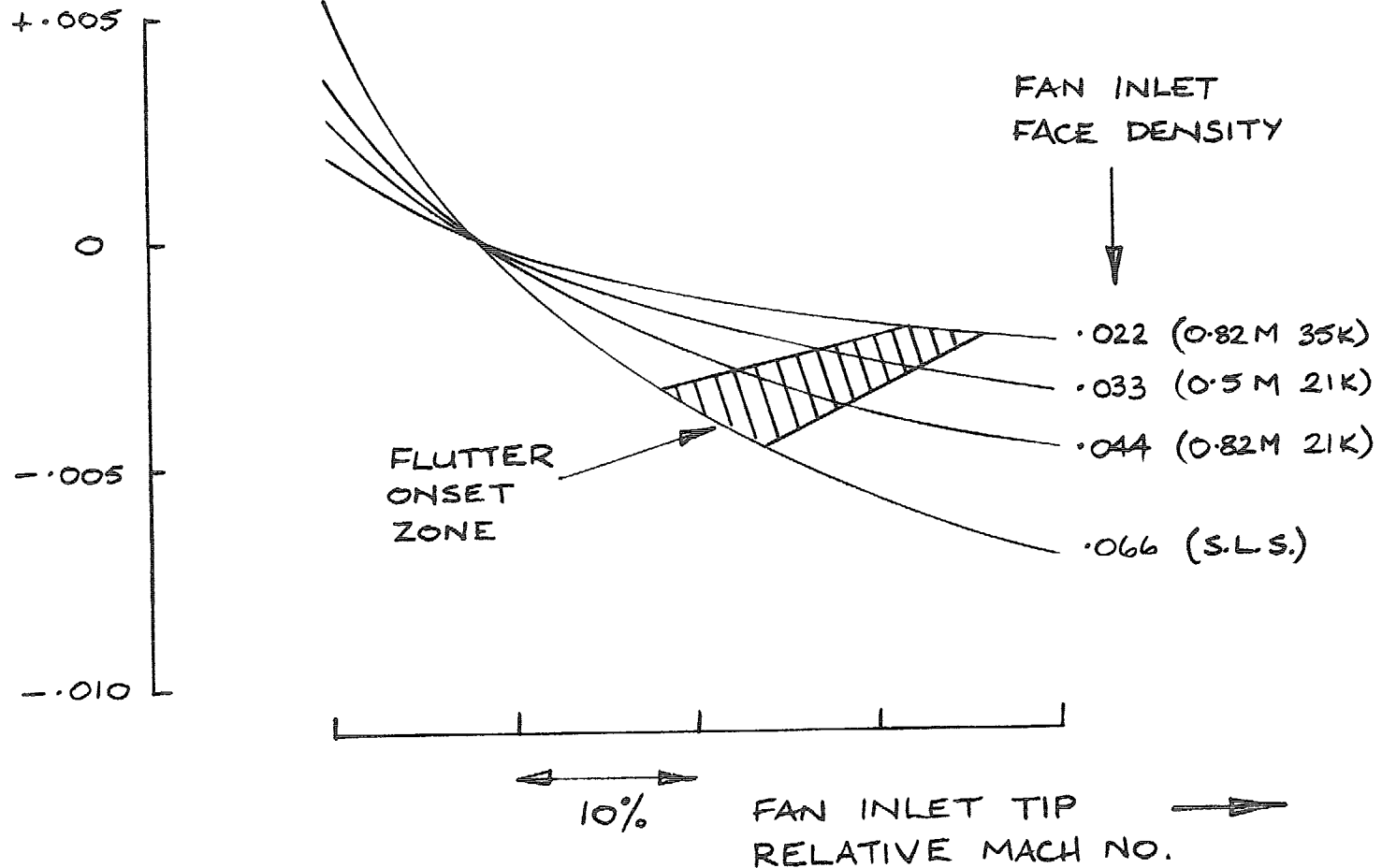


FIG. 14. Density correlation of fan flutter test data.

# AERODYNAMIC DAMPING



Printed in England for Her Majesty's Stationery Office by J. W. Arrowsmith Ltd., Bristol BS3 2NT  
 Dd. 290278 KS 12/76

FIG. 15. Effect of density on aerodynamic damping four-diameter second family mode.

© Crown copyright 1977

HER MAJESTY'S STATIONERY OFFICE

*Government Bookshops*

49 High Holborn, London WC1V 6HB  
13a Castle Street, Edinburgh EH2 3AR  
41 The Hayes, Cardiff CF1 1JW  
Brazennose Street, Manchester M60 8AS  
Southey House, Wine Street, Bristol BS1 2BQ  
258 Broad Street, Birmingham B1 2HE  
80 Chichester Street, Belfast BT1 4JY

*Government publications are also available  
through booksellers*